The influence of incorporating cobalt (Co) and indium (In) co-dopants on the structural and optical properties of ZnO nanoparticles

Mpho W. Maswanganye[1], Koena E. Rammutla[1], Thuto E. Mosuang[1*], Bonex W. Mwakikunga[2], Sone T. Bertrand[3], Malik Maaza[3]

[1]Department of Physics, University of Limpopo, Private Bag x1106, Sovenga 0727, South Africa
[2]DST/CSIR National Centre for Nano - Structured Materials, P O Box 325, Pretoria 0001, South Africa
[3]Materials Research Department, iThemba labs, P O Box 722, Somerset West 7129, South Africa

[*]Corresponding author, Tel: (+27) 15 268 3576; E-mail: Thuto.Mosuang@ul.ac.za

Received: 18 April 2016, Revised: 16 September 2016 and Accepted: 14 October 2016

DOI: 10.5185/amlett.2017.6876
www.vbripress.com/aml

Abstract

Co and In co-doped nanopowders of ZnO as well as In and Co singly doped ZnO were successfully prepared using sol-gel method. The synthesized samples were characterized using x-ray diffraction (XRD), UV-vis spectroscopy (UV-vis), Raman spectroscopy (RS), Transmission Electron Microscopy (TEM) and Energy Dispersive Spectroscopy (EDS). The effects of In and Co co-doping on the structural and optical properties were investigated. XRD results showed no peaks associated with In^{3+} or Co^{2+} ions indicating that In^{3+} and Co^{2+} ions substituted for Zn^{2+} ions in the ZnO wurtzite structure, this was corroborated by the EDS results. Doping ZnO nanoparticles with In and Co significantly reduced the grain sizes whereas the lattice parameters were not significantly affected. TEM results confirmed that the nanoparticles were spherically shaped. Raman spectroscopy also confirmed that the ZnO nanoparticles were of a wurtzite hexagonal structure. Single doping reduced the energy band gaps and co-doping reduced them even further. Copyright © 2016 VBRI Press.

Keywords: ZnO nanoparticles, sol-gel method, co-doping, structural properties, optical properties.

Introduction

ZnO is an n-type semiconductor material with a hexagonal wurtzite structure having a wide energy band gap of 3.36 eV and a large excitation binding energy of 60 meV. It has a wide range of resistivity, high transparency at room temperature **[1]**, high electron hall mobility, good chemical and thermal stability under operation conditions **[1, 2]**. This material is widely used in a variety of applications such as opto-electronic devices **[3]**, light emitting diodes **[3]**, flat panel displays **[5]**, surface acoustic wave devices **[6]**, chemical and gas sensors **[7]** and solar cells **[8]**.

Nanostructured materials are quite interesting and they are being investigated because of their diverse properties compared to those of bulk materials **[9]**. Previous work has shown that the functionality of ZnO nanostructured materials depends on their size, shape and structural aspect. These factors are mostly influenced by the method of preparation **[10-12]**. Different methods such as chemical vapor deposition (CVD) **[13]**, physical vapor deposition (PVD) **[14]**, hydro thermal and sol-gel method **[15]** have been used to synthesize the undoped and doped ZnO nanoparticles. It has also been reported that doping ZnO nanoparticles with a controlled amount of impurities can affect its structural, electrical and optical properties and hence great effort has been devoted in doping ZnO nanoparticles with impurities such as Cu, Al, In, Sb, Ga, Fe, Co, Ni, etc. **[16]**. Combinational doping ZnO nanoparticles with more than one element has also been reported to enhance its properties even further. Ji-ling Song et al. **[17]** reported that combinational doping ZnO with Y and Cd can improve its structural and optical properties, while S.S. Abdullahi et al. **[18]** reported on the co-doping of ZnO with Mn and Co to be affecting the structural and optical properties of the ZnO nanoparticles. Advancements in photocatalysis and solar cells due to co-doping ZnO are already being reported on **[19, 20]**. Y.S. Malghe and A.B. Lavand **[21]** further showed that doping and coupling enhances photocatalytic activity in the ZnO nanocomposites. Cobalt (Co) has been reported to reduce the grain size of ZnO nanoparticles and also enhances its optical properties by narrowing the energy band gap **[22]**. Furthermore, indium (In) has been reported to enhance the electrical and optical properties of ZnO nanoparticles **[23]**. At present there are only few reports on the combinational doping of ZnO nanoparticles with In and Co and not much is known about their effects on the ZnO properties.

In this work focus will be on investigating the structural and optical properties of ZnO doped with 5 wt. % of Co, 5 wt. % In doped and combinational doping i.e. 2.5wt. % In / 2.5 wt. % Co prepared using sol-gel method for future possible gas sensing applications.

Copyright © 2016 VBRI Press

Experimental

Material synthesis and characterizations

The undoped, single doped and double-doped ZnO nanoparticle samples were synthesized using zinc acetate dihydrate ($C_4H_6O_4Zn{\cdot}2H_2O$), ethanol (C_2H_6O), ethanolamine (C_2H_7NO), cobalt (II) nitrate hexahydrate ($CoN_2O_6{\cdot}6H_2O$) and indium (III) nitrate hydrate ($InN_3O_9{\cdot}xH_2O$). The water soluble salts, i.e. cobalt (II) nitrate hexahydrate and indium (III) nitrate hydrate were used as sources of Co and In metal dopants. All the chemicals used were standard chemicals purchased from Sigma-Aldrich. Single doped ZnO nanoparticles with Co and In were prepared at 5 wt. %, the co-doped ZnO nanoparticles samples were prepared at 2.5 wt. % of each dopant in order to obtain a summed up 5 wt. %.

When preparing the undoped ZnO nanoparticles 0.2 M of zinc acetate dihydrate solution was mixed with 0.2 M of ethanol in order to obtain homogeneity, this was done at a continuous stirring. For the single doped ZnO nanoparticles, cobalt (II) nitrate hexahydrate or indium (III) nitrate hydrate were added into 0.2 M of zinc acetate dihydrate solution and for the co-doped ZnO nanoparticles, cobalt (II) nitrate hexahydrate and indium (III) nitrate hydrate were added simultaneously into 0.2 M of zinc acetate dihydrate solution. All these solutions were then mixed with 0.2 M of ethanol in order to obtain homogeneity and this was done at a continuous stirring. 0.2 M of ethanolamine was then added into all the solutions as a stabilizer and all the solutions were stirred at 70 ^{o}C for 2 hours. The precipitates formed were collected using filter paper, and dried at 100 ^{o}C for 1 hour in a hot air oven. All the samples were annealed at 500 ^{o}C for 1 hour. After annealing, all the samples were subjected to characterization using XRD, TEM, Raman spectroscopy and UV-vis spectroscopy.

Results and discussion

Fig. 1 shows the XRD patterns of all the prepared samples. All the samples were found to have the ZnO hexagonal wurtzite structure with peaks observed at 2θ = 31.77°, 34.43°, 36.27°, 47.56° and 56.63° corresponding to the (100), (002), (101), (102) and (110) planes respectively (JCPDS No.36-1451). No peaks associated with Co or In were detected in the XRD patterns indicating that Co^{2+} and In^{3+} ions successfully substituted for the Zn^{2+} ions. This implies that Co^{2+} and In^{3+} ions were successfully incorporated into the Zn^{2+} ions sites in the ZnO crystal structure. The lattice parameters a = b and c for the undoped and doped ZnO nanoparticles were calculated using the planes (100) and (002) and the calculated values were found to be similar to the reported values of the bulk ZnO (JCPDS No.36-1451); the results are tabulated in **Table 1.**

The average grain sizes of the undoped and doped ZnO nanoparticles were estimated by Scherrer's equation and are also presented in **Table 1.** From the table, it can be seen that incorporation of Co^{2+} and In^{3+} ions into the ZnO nanoparticle structure reduced the average grain sizes of the ZnO nanoparticles. Simultaneous doping with both indium and cobalt reduced the grain sizes even further.

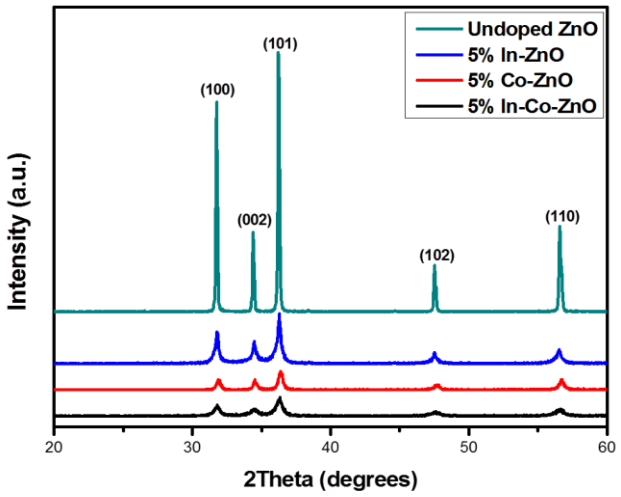

Fig. 1. XRD patterns: undoped and doped ZnO, 5% of Co, 5% of In doped ZnO and 5% of In-Co double-doped ZnO nanoparticles annealed at 500 °C.

The strains were determined for all the samples using the equation:

$$\varepsilon = \frac{\beta_{(hkl)} \cos\theta}{4 \sin\theta}$$

and the values were found to be inversely proportional to the grain size as seen in **Table 1.** The bond lengths of the undoped and the doped ZnO nanoparticles were determined using equation:

$$L = [\frac{a^2}{3} + \left(\frac{1}{2} - u\right)^2 c^2],$$

where the u parameter for the wurtzite crystal structure is defined by:

$$u = \frac{a^2}{3c^2} + 0.25.$$

The bond lengths of the undoped and the doped ZnO nanoparticles are shown in **Table 1.** It can be observed that the bond lengths of the ZnO nanoparticles contract a little with introduction of dopants which indicates the presence of Co and In in the ZnO structure.

Table 1. Lattice parameters, average grain size, average strain and bond lengths.

Sample Name	Lattice parameters a = b (Å)	c (Å)	D (nm)	ε (× 10^{-3})	L (Å)
Undoped-ZnO	3.2500	5.2070	52.2653	1.9509	3.9122
5% Co-ZnO	3.2370	5.1861	20.1338	5.0575	3.8809
5% In-ZnO	3.2480	5.1953	21.7272	4.7072	3.9034
5%In-Co-ZnO	3.2474	5.1939	13.1658	7.8151	3.9016

Fig. 2 shows the TEM and EDS images of 5% Co, 5% In and 5% In-Co double-doped ZnO nanoparticles samples. All the prepared samples are found to be spherically shaped and in **Fig. 2 (b)** big rods can be seen alongside the spherical nanoparticles. These rods are basically created when spherical nanoparticles come together and as such smaller particles can be seen inside

Copyright © 2016 VBRI Press

the rods. Similar observations were reported by Xu et al. **[24]**. The EDS images confirm that Co and In were successfully incorporated into the ZnO nanoparticle matrix.

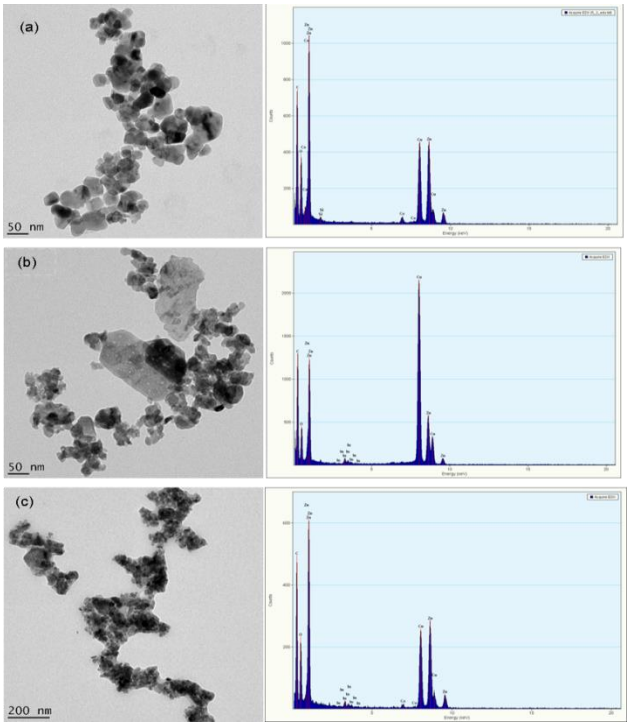

Fig. 2. TEM and EDS images of (a) 5% Co-ZnO, (b) 5% In –ZnO and (c) 5% In-Co-ZnO.

The vibrational properties of the undoped and doped ZnO nanoparticle samples were investigated using the excitation wavelength of 514 nm at room temperature. The group theory predicts that the ZnO wurtzite hexagonal structure of a space group C_{6v}^4 will indicate the phonon modes near the centre of Brillouin zone given by the equation $\Gamma = A_1 + 2B_1 + E_1 + 2E_2$. A_1, E_1 and $2E_2$ are Raman active modes and $2B_1$ is the forbidden mode of ZnO. A_1 and E_1 are polar and they are split into two; being transverse optical (TO) and longitudinal optical (LO) phonons and E_2 is divided into E_2^{low} and E_2^{high} **[25]**. E_2^{high} is assigned to the vibration of oxygen atoms in the ZnO. From **Fig. 3**, four active Raman modes can be observed with peaks at 329.1, 377.4, 434.9 and 577.9 cm^{-1} which are consequently assigned to the modes E_2^{high}-E_2^{low}, A_1(TO), E_2^{high} and E_1 respectively. Previous studies have suggested that the peak at 434.9 cm^{-1} confirms that the nanoparticles are of a ZnO wurtzite hexagonal crystal structure **[26-28]**. The peak at 577.9 cm^{-1} belongs to point defects such as oxygen vacancies (V_O), zinc interstitials (Zn_i) and/or free carriers as reported in several articles **[28, 29]**.

The optical absorption spectra of the undoped and doped ZnO nanoparticles were recorded in order to investigate the optical properties of samples and the results are presented in **Fig. 4.** For the nanoparticles doped with Co three additional absorption peaks are observed between 550-700 nm.

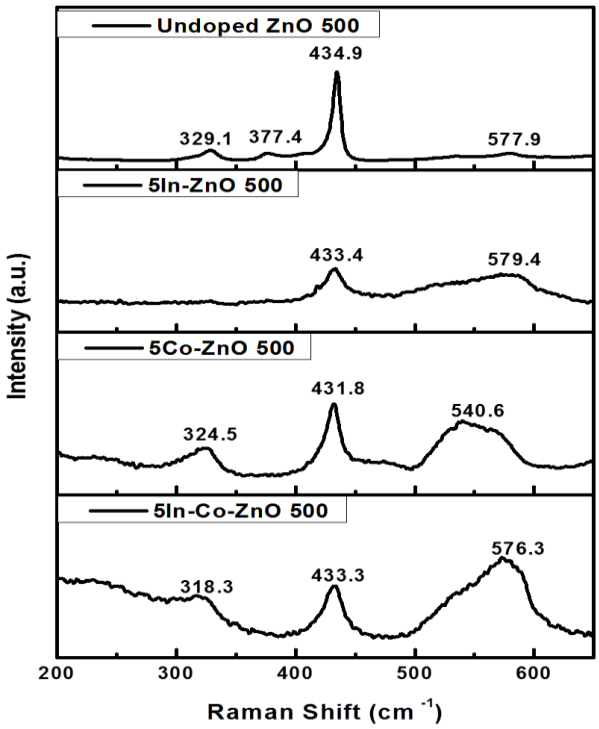

Fig. 3. Raman spectroscopy of undoped and doped ZnO, 5% of Co, 5% In and 5% of In-Co co-doped ZnO nanoparticles.

These peaks can be attributed to $^4A_2(F) \rightarrow {}^2A_1(G)$, $^4A_2(F) \rightarrow {}^4T_1(P)$ and $^4A_2(F) \rightarrow {}^2E(G)$ transitions which suggest that the tetrahedrally coordinated Co^{2+} ions have successfully substituted for Zn^{2+} ions in the hexagonal ZnO wurtzite structure **[30]**.

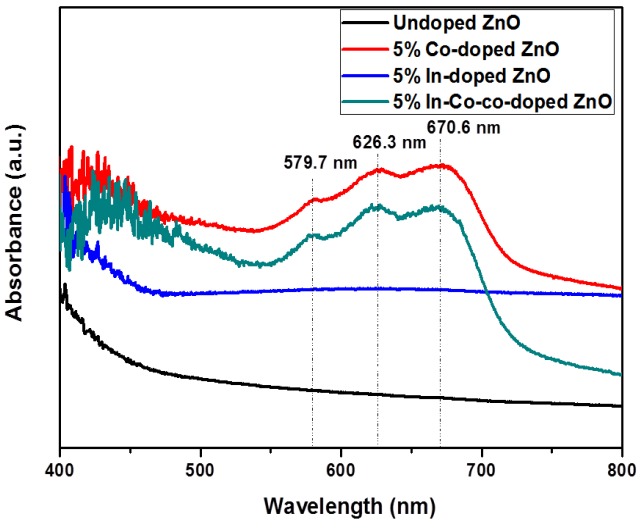

Fig. 4. Optical Absorbance spectra of undoped doped ZnO, 5% of Co, 5% In and 5% of In-Co co-doped ZnO nanoparticles.

The optical band gap (E) of the samples was calculated using the following equation **[31]**

$$E = {}^{hc}/_{\lambda}$$

where, h is the Planck constant, c is the speed of light, λ is the cut-off wavelength. The cut-off wavelength is

Copyright © 2016 VBRI Press

determined by extrapolating the straight line portion of the plot to intercept the wavelength axes. These cut-off wavelengths are associated with the absorption edges. The energy band gap values are presented in **Table 2**. It can also be observed that the values of the calculated energy band gap are smaller compared to the reported value of the bulk ZnO **[32]**. This could be due to the fact that nanostructured materials have different properties compared to their bulk materials. In addition a red shift has been observed between the undoped ZnO nanoparticles and the doped ZnO nanoparticles. Ando et al. **[33]** argued that the red shift could be attributed to the fact that Co^{2+} and In^{3+} ions substituted the Zn^{3+} ions in the crystal lattice. Doping ZnO nanoparticles with Co or In reduces the band gap of the material. But In-Co combinational doping reduces the band gap tremendously as shown in **Table 2**.

Table 2. Energy band gap in undoped, 5% Co, In, In-Co doped ZnO.

Sample Name	E_g (eV)
Undoped-ZnO	2.91
5% Co-ZnO	2.22
5% In-ZnO	2.70
5%`In-Co-ZnO	2.07

Conclusion

The undoped ZnO, 5% In, 5% Co doped and 5% In-Co co-doped ZnO nanoparticles were successfully prepared using sol-gel method. All the prepared samples were found to be having a hexagonal wurtzite crystal structure. In^{3+} and Co^{2+} were substitutionally incorporated into the Zn^{2+} ion sites of the ZnO nanoparticle lattice structure. Doping ZnO nanoparticles with In and Co reduced the grain sizes and the energy band gap. Simultaneous doping reduced the grain sizes and energy band gaps even further. TEM results confirmed that the nanoparticles were spherically shaped while the EDS also confirmed that In^{3+} and Co^{2+} are incorporated into the ZnO hexagonal structure. Raman spectroscopy confirmed that the prepared ZnO nanoparticles were of a wurtzite hexagonal structure.

Acknowledgements

The authors would like to thank the UL, NRF, IBSA, and iThemba Labs for financial support. UWC, US and CSIR acknowledged for experimental resources.

Author's contributions

Conceived the plan: KE, TE, M; Performed the experiments: MW, BW, ST, M; Data analysis: MW, KE, TE, ST, M; Wrote the paper: MW, KE, TE. Authors have no competing financial interests.

References

1. Pearton, S.; Norton, D.; Ip, K.; Heo, Y.; Steiner, T.; *J. Vac. Sci. Technol. B.* **2004**, *22*, 932. **DOI:** 10.1116/1.1714985
2. Mankad, V.H.; Gupta, S.K.; Jha, P.K.; *Adv. Mater. Lett.* **2016,** *7*, 246. **DOI:** 10.5185/amlett.2016.6147
3. Gruzintsev, A.; Volkov, V.; Yakimov, E.; Semicond. **2003**, *37*, 259. **DOI:** 10.1134/1.1561514
4. Kim, H.; Horwitz, J.; Kim, W.; Makinen, A.; Kafafi, Z.; Chrisey, D.; *Thin Solid Films*. **2002**, *420*, 539. **DOI:** 10.1016/S0040-6090(02)01016-7
5. Chen, M.; Pei, Z.; Sun, C.; Gong, J.; Huang, R.; We, L.; *Mater. Sci. Eng. B.* **2001**, *85*, 212. **DOI:** 10.1016/S0921-5107(01)00584-0
6. Lee, J.; Lee, H.; Seo, S.; Park, J.; *Thin Solid Films.*, **2001**, 398, 641. **DOI:** 10.1016/s0040-6090(01)01332-3
7. Bohle, J.;.Spina, C.; *J. Phys. Chem. C.*, **2010**, *114*, 18139. **DOI:** 10.1021/jp108391e
8. Al-Kahlout, A.; *Thin Solid Films*., **2012**, *520*, 1814. **DOI:** 10.1016/j.tsf.2011.08.095
9. Klingshirn, C.; Fallert, J.; Zhou, H.; J.Sartor, Thiele, C.; Maier-Flaig, F.; Schneider, D.; Kalt, H.; *Phys. Status Solidi. B.* **2010**, *247*, 1424. **DOI:** 10.1002/pssb.200983195
10. Kim, S.Y.; Lee, I.S.; Yeon, Y.S.; Park, S.M. Song, J.K.; *Bull. Korean Chem. Soc.*, **2008**, *29*, 1960. **DOI:** 10.5012/bkcs.2008.29.10.1960
11. Woo, B.; Chen, W.; Joly, A.; Sammynaiken. R.*; J. Phys. Chem. C.* **2008**, *112*, 14292. **DOI:** 10.1021/jp803649k.
12. Dutta, R.; Sharma, P.; Bhargava, R.; Kumar, N.; Pandey, A.C.; *J. Phys. Chem B.* **2010**, *114*, 5594. **DOI:** 10.1021/jp1004488
13. Nishino, J.; Kawarada, T.; Ohshio, S.; *J. Mater. Sci. Lett.* **1997**, *16*, 629. **DOI:** 10.1023/a: 1018511131738
14. Sathyal, M.; Claude, A.; *Advanced in Applied Science Research*, **2010**, *3*, 2591. **DOI:** 10.1002/app.31282
15. Rokn-Abadi, M.; Behdani, M.; Arabshahi H.; Hosseini, N.; *International Review of Physics*. **2009**, *12*, 103.
16. Poloju, M.; Reddy, M.; ICANMEET, India, **2013**. **DOI:** 10.1109/icanmeet.2013.6609269
17. Song, J.; Zheng, J.; Zhao, Z; Zhou, B.; Lian, J.; Trans. *Nonferrous Met. Soc*. **2013**, *23*, 2336. **DOI:** 10.1016/s1003-6326(13)62738-7
18. Abdullahi, S.S.; Köseoglu, Y.; Güner, S.; Kazan, S.; Kocaman, B; Ndikilar, C.E.; *Superlattices Microstruct.* **2015**, *83*, 342. **DOI:** 10.1016/j.spmi.2015.03.021
19. Pan, Z.; Luo, J.; Tian, X.; Wu, S.; Chen, C.; Deng, J.; Xiao, C.; Hu, G.; Wei, Z.; *J. Alloys Compd.*, **2014**, *583*, 32. **DOI:** 10.1016/j.jallcom.2013.06.192
20. Lavand, A. B.; Malghe, Y. S.; *Adv. Mater. Lett.*, **2016**, *7*, 181. **DOI**: 10.5185/amlett.2016.5974
21. Malghe, Y.S.; Lavand, A.B.; *Adv. Mater. Lett*., **2016**, *7*, 239. **DOI:** 10.5185/amlett.2016.6130
22. Li, P.; Wang, S.; Li, J.; Wei, Y.; J. Lumin, **2012**, *132*, 220. **DOI:** 10.1016/j.jlumin.2011.08.019
23. Huang, Y.; Zhang, Y.; Gu, Y.; Bai, X.; Qi, J.; Liao Q.; Liu J.; *J. Phys. Chem. C.*, **2007**, *111*, 9039. **DOI:** 10.1021/jp0666030
24. Xu, L.; Zhang, H.; Shen, K.; Xu, M.; Xu, Q.; *J Supercond Nov Magn.*, **2012**, *25*, 1951. **DOI:** 10.1007/s10948-012-1535-z
25. Du, Y.; Zhang, Y.; Sun, L.; Yan, C.; *J. Phys. Chem. C.*, **2008**, *112*, 12234. **DOI:** 10.1021/jp802958x
26. Romcevic, N.; Kostic, R.; Romcevic, M.; Hadzic, B.; Kuryliszyn-Kudelska, I.; Dobrowolski, W.; Narkiewicz, U.; Sibera, D.; *Acta. Phys. Pol. A*, **2008**, *114*, 1323.
27. Devaraj, R.; Karthikeyan, K.; Jeyasubramanian, K.; *Appl. Nanosc.*, **2012**, *3*, 37. **DOI:** 10.1007/s13204-012-0072-1.
28. Yang, R.; Tripathy, S.; Yuntao, L.; Sue, H.-J.; *Chem. Phys. Lett.* **2005**, *411*, 150. **DOI:** 10.1016/j.cplett.2005.05.125
29. Schumm, M. ZnO based semiconductors studied by Raman spectroscopy: semimagnetic alloying, doping and nanostructures, PhD Thesis, Julius Maximilians–Universitat Wurzburg, **2008**.

Copyright © 2016 VBRI Press

30. Yang, L.; Tang, Y.; Hu, A.; Chen, X.; Liang, K.; *Zhang, L. Physica B.*, **2008**, *403*, 2230.
DOI: 10.1016/j.physb.2007.12.013
31. Weakliem, H.; *J. Phys. Chem***. 1962**, *36*, 2117.
DOI: 10.1063/1.1732840
32. Xie, O; McCourt, F; Nanotechnology Engineering NE 320L Lab Manual, University of Waterloo, Waterloo, **2008**, 23.
33. Ando, K.; Saito, H. Jin, Z.; Fukumura, T.; Kawasaki, M.; Matsumoto Y.; Koinuma, H.; *J. Appl. Phys.* **2001**, *89*, 7284.
DOI: 10.1063/1.1356035